Developmental Cell, Volume *42*

Supplemental Information

Fgf8 Expression and Degradation of Retinoic Acid Are Required for Patterning a High-Acuity Area in the Retina

Susana da Silva and Constance L. Cepko

Figure S1, related to Figure 1

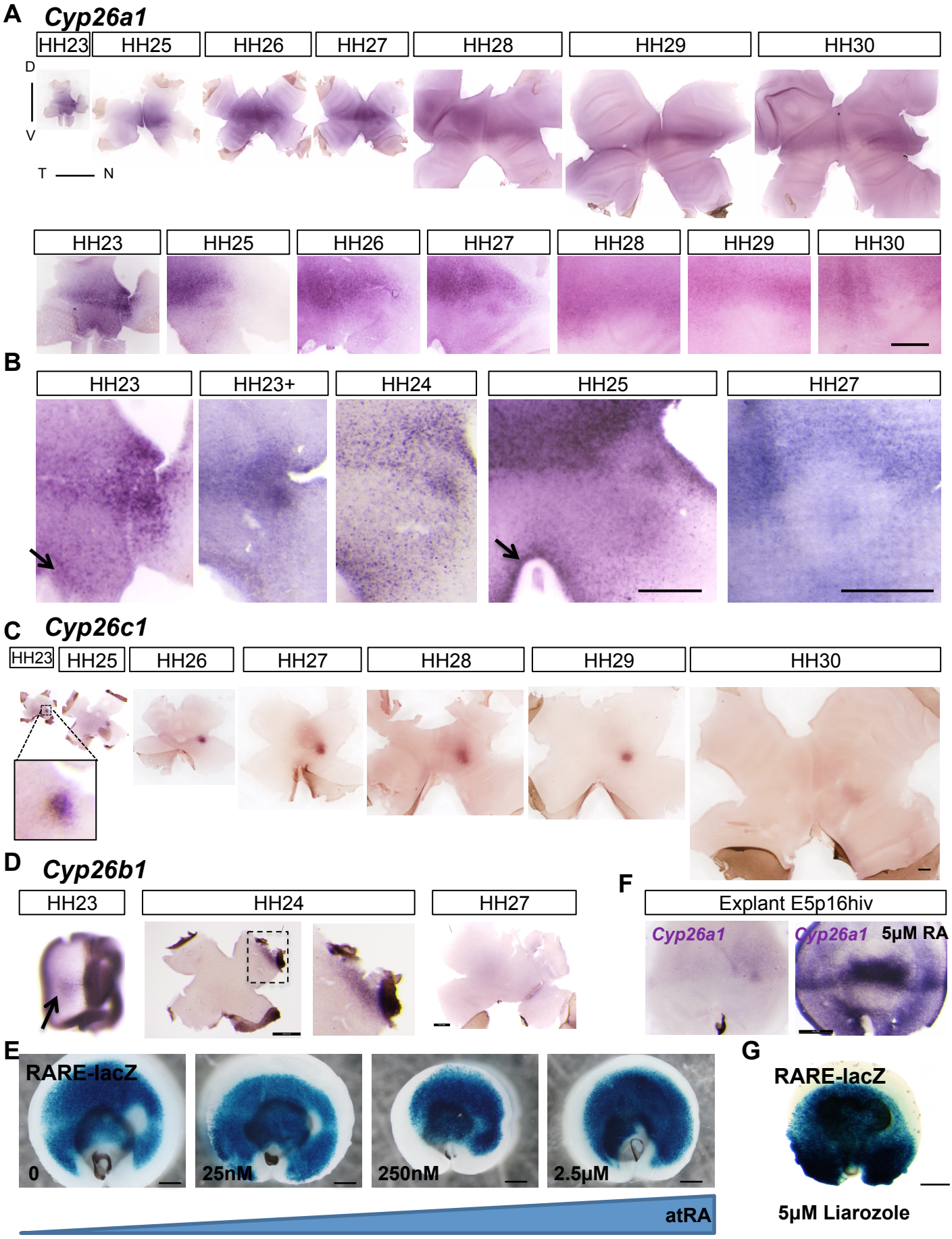

Figure S1- Time course of expression of RA degrading enzymes, Cyp26a1, Cyp26c1 and Cyp26b1, during retinogenesis and RARE activity following addition of atRA, related to Figure 1.
(A) Flat mount chromogenic ish of Cyp26a1 from HH23 to HH30. Note the dynamic expression of the bull's eye domain, which ceases after HH27, more apparent in the magnified images. The stripe domain is maintained at least until HH30. (B) Further magnification focusing on the bull's eye domain of Cyp26a1, illustrating the transient expression of this domain. Note that Cyp26a1 is also expressed along the optic fissure (arrows). (C) Flat mount ish for Cyp26c1 from HH23 to HH30. Note the discrete circular domain of Cyp26c1 expression in a central spot and slightly nasal to optic nerve head at HH23 that lasts at least until HH30. This pattern seems to expand with time and fades after HH29. (D) Whole mount and flat mount ish for Cyp26b1 at stated time points. At HH23 a faint domain of expression was observed in the nasal pole of the retina, arrow. At HH24 some expression was still detected at the most peripheral retina of the nasal region and at HH27 no expression was detected. (E) Dose-dependent response of the RA reporter to increasing amounts of atRA added in the culture medium of E5 plus 2div explants. Note the gradual loss of the RA-signaling free spot with higher doses of atRA. (F) Retina explant cultured for 16 hours *in vitro* and processed for Cyp26a1 ish. Note the increase of Cyp26a1 expression throughout the whole retina in response to 5μM atRA added to the medium. Both control and treated retinas were processed together and stained for the same amount of time. (G) RARE-reporter response of E5 plus 2div explant incubated with 5μM of Liarozole, a Cyp26s proteins inhibitor. Note the loss of the RARE-signaling-free spot. Scale bar, 500μm. D, dorsal; V, ventral; N, nasal; T, temporal. All images are oriented consistently.

Figure S2, related to Figure 1

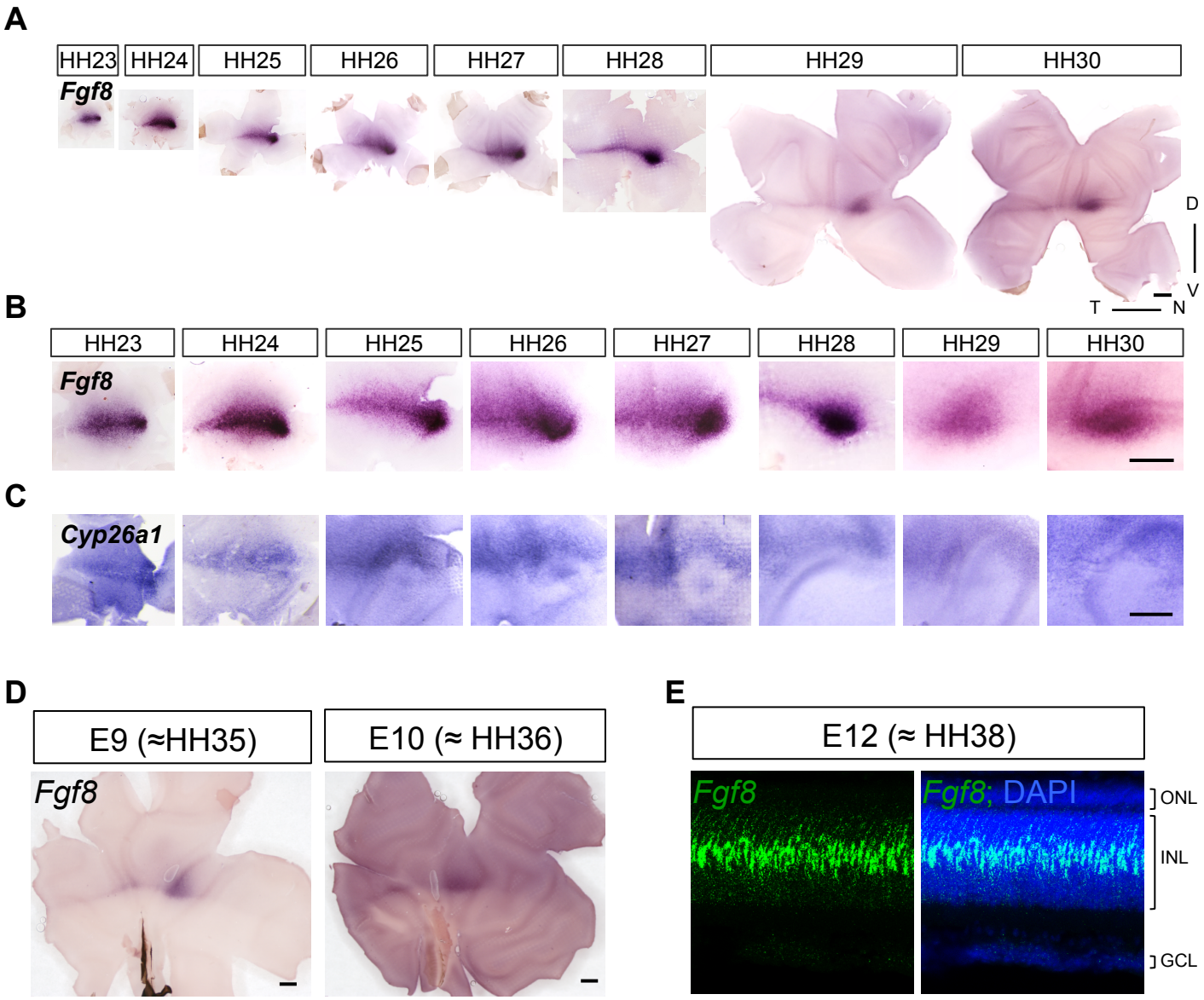

Figure S2 – Time-course expression of Fgf8 during retinogenesis, relative to Cyp26a1, related to Figure 1
(A) Flat mount chromogenic ish of Fgf8 from HH23 to HH30. Note the presence of a spot located centrally and nasal to the optic nerve head and a stripe across the equator. (B) Fgf8 ish time course focusing on the spot domain of expression and (C) relationship with Cyp26a1 bull's eye domain. Note that the Fgf8 spot increased in size over time. The Fgf8 spot became stronger with time until it reached the peak of intensity at HH27/HH28, coincident with the loss of the Cyp26a1 bull's eye. (D) Fgf8 transcripts were still detected at HH35-36 in a patterned manner. (E) Fish for Fgf8 counterstained with DAPI on a HH38 retina cross section showed expression of Fgf8 in the central retina in a subset of cells with their cell bodies located in the center of the INL, likely Mueller glial cells. Scale bar, 500μm in (A), (B), (C) and (D) and 50μm in (E). D, dorsal; V, ventral; N, nasal; T, temporal; ONL, outer nuclear layer; INL, inner nuclear layer; GCL, ganglion cell layer.

Figure S3, related to Figure 2

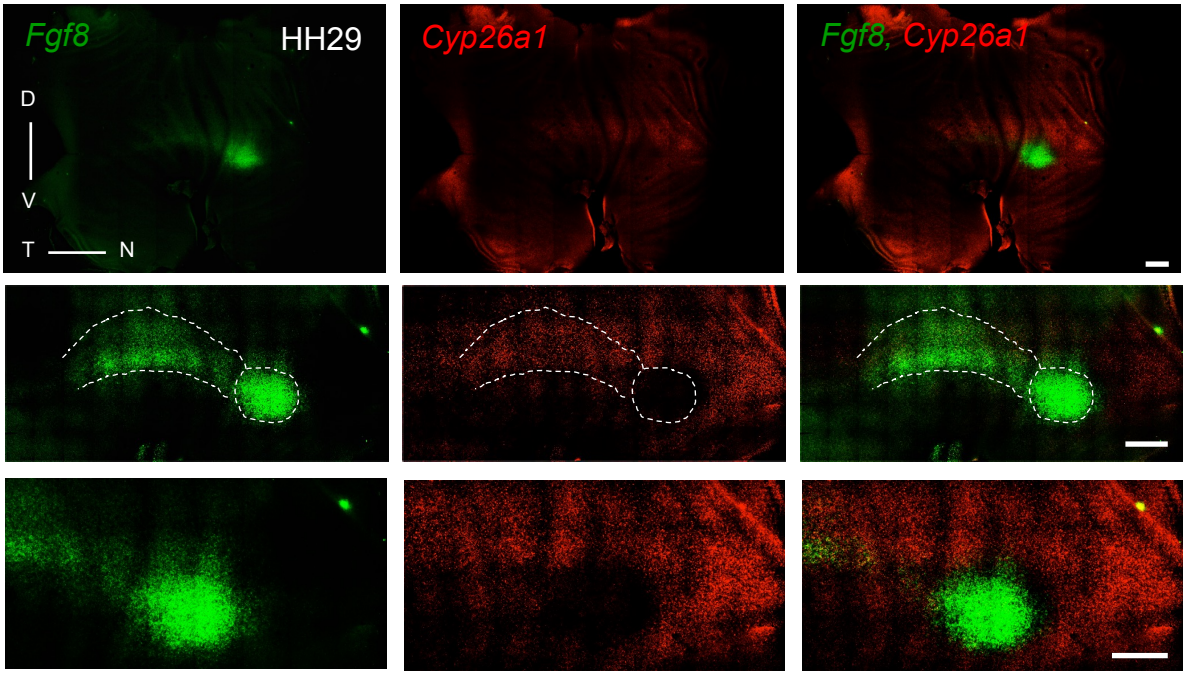

Figure S3 – Spatial correlation between Fgf8 and Cyp26a1 at HH29, related to Figure 2
Flat mount fish of a HH29 chick retina probed for Fgf8, in green, and Cyp26a1, in red. High magnification images demonstrate the partial spatial co-localization between both transcripts in the stripe domain along the equator of the retina. However the Fgf8 expression does not co-localize with Cyp26a1 expression in his spot domain but rather fills in the Cyp26a1-negative circular region. Scale bar, 500μm. D, dorsal; V, ventral; N, nasal; T, temporal.

Figure S4, related to Figure 4

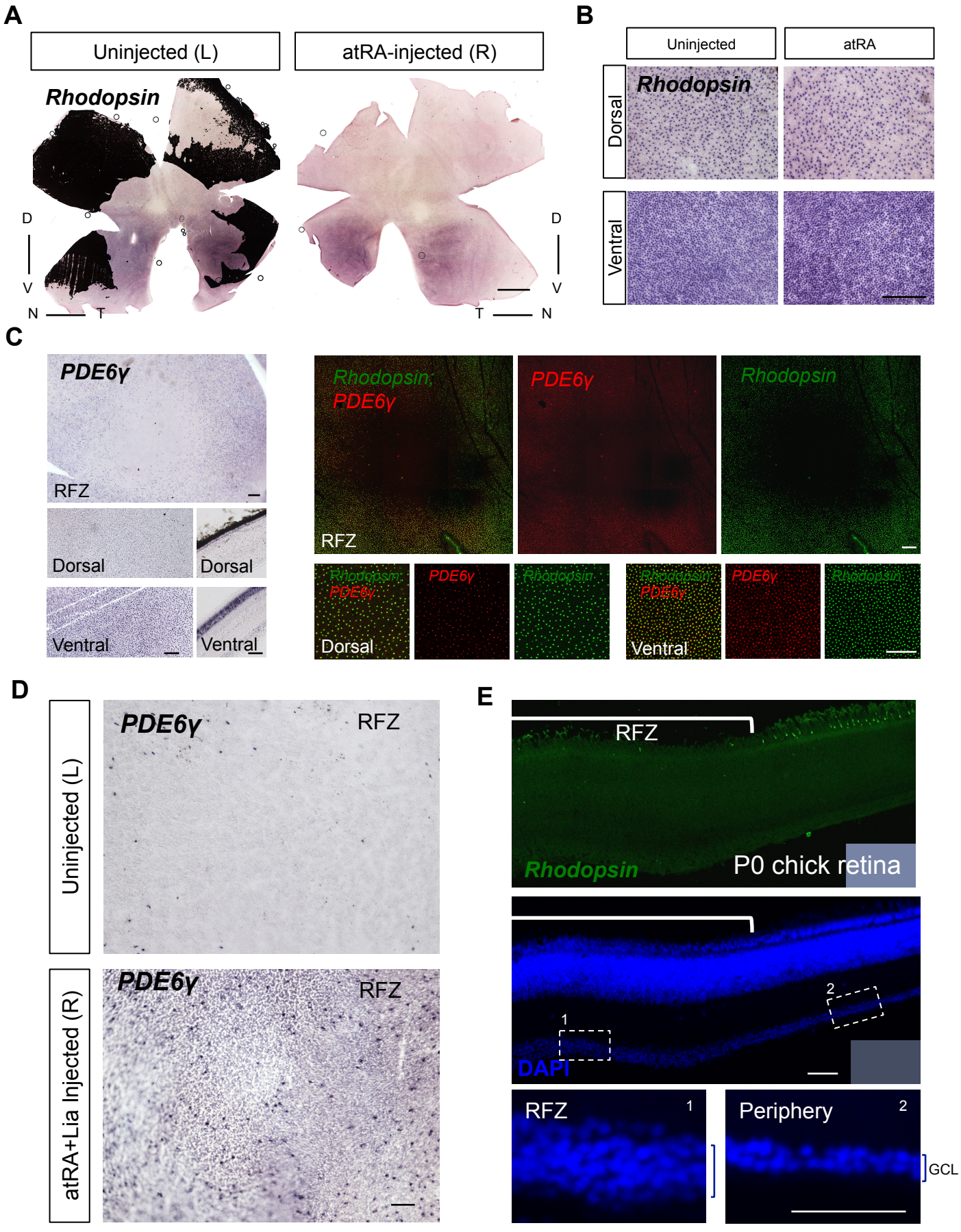

Figure S4 – Pharmacological manipulation of RA signaling at HH25 affects the HAA by disturbing the RFZ, related to Figure 4

(A) Retina injected in vivo with atRA at HH25, harvested at E19, analyzed for Rhodopsin ish and the matching uninjected L eye of the same embryo. Note that overall the two retinas look alike, their size was similar and the high-ventral to low-dorsal gradient of rhodopsin expression was present in both. Some RPE is still present in the L retina. (B) Images of dorsal and ventral regions from an uninjected and atRA-injected retina at HH25 and processed for rhodopsin ish at E19. (C) Validation of PDE6γ marker as a specific rod marker. Single chromogenic ish on flat mount and cross sections of E19 chick retina confirmed the presence of a RFZ and a high-ventral to low-dorsal gradient of rods. Flat mount double fish for rhodopsin, in green, and PDE6γ, in red, shows 100% co-localization between the two probes. (D) Flat mount ish with PDE6γ probe in atRA+Liarozole-treated retinas and uninjected L eye revealed induction of PDE6γ positive cells in the RFZ. (E) Fish on a cross section of P0 chick retina for rhodopsin and counterstained with DAPI. Note the presence of the RFZ and the increase in GCL thickness beneath the RFZ versus outside the RFZ, more apparent in the high magnifications of the corresponding boxed areas, 1 and 2, respectively. Scale bar, 2mm in (A), 100μm in (B), (D) and 50μm in (C), (E). D, dorsal; V, ventral; N, nasal; T, temporal; GCL, ganglion cell layer.

Figure S5, related to Figure 5

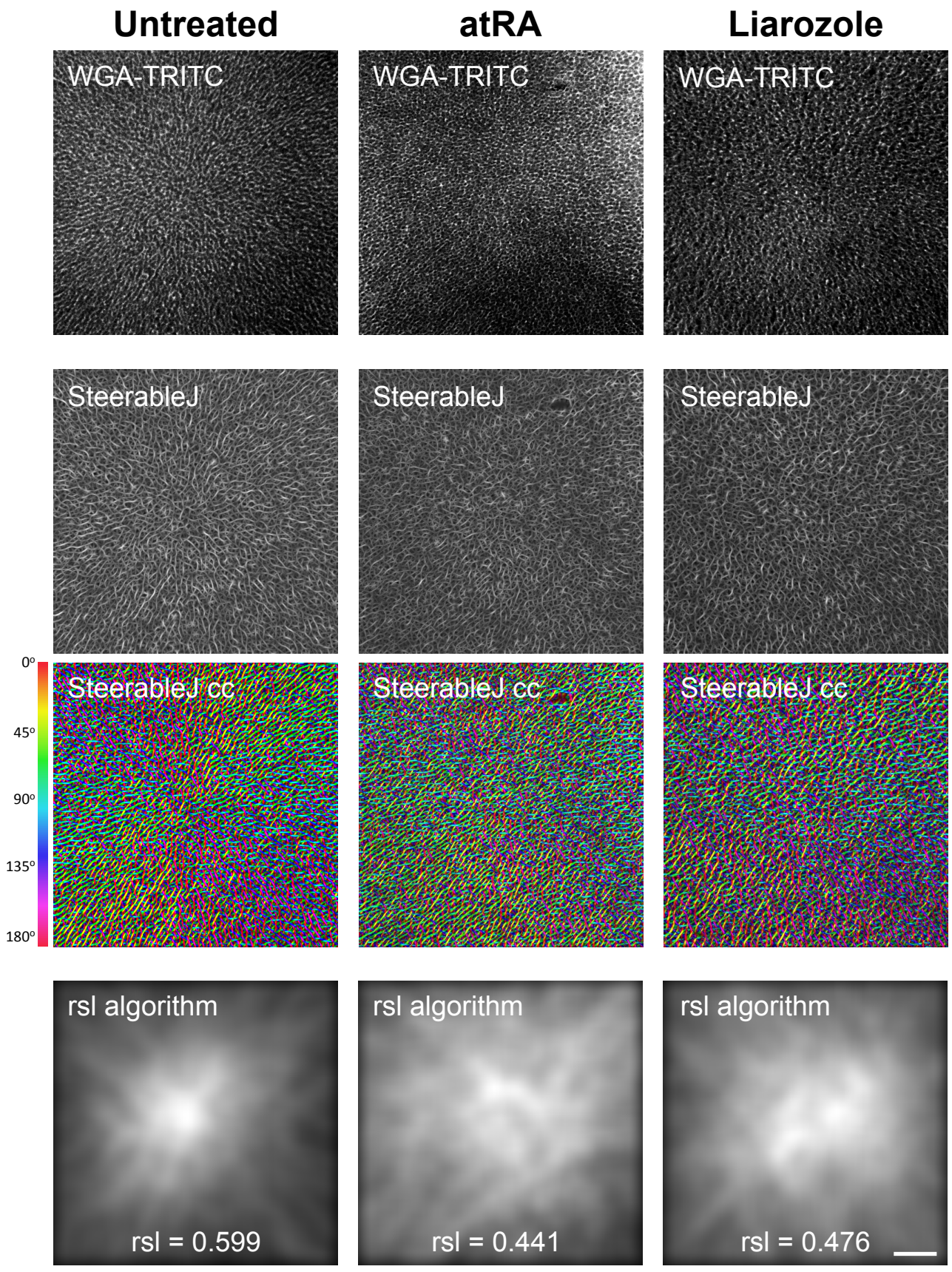

Figure S5 – Pharmacological manipulation of RA signaling at HH25 affects the HAA, by disturbing the aster structure, related to Figure 5

Representative images of the aster structure visualized by WGA-TRITC staining, top panels, in untreated, atRA- and Liarozole-treated retinas. Corresponding SteerableJ transformations and color-coded outputs of the examples are shown. Note the loss of radial organization of aster structure in atRA- and Liarozole-injected retinas in relation to untreated retina. Application of the rsl algorithm to the same examples shows a reduced rsl value in treated compared to untreated retina. Corresponding rsl values for each retina is shown (see Figure 5G scatter plot for quantification and statistical analysis). Scale bar, 50μm.

Figure S6, related to Figure 6

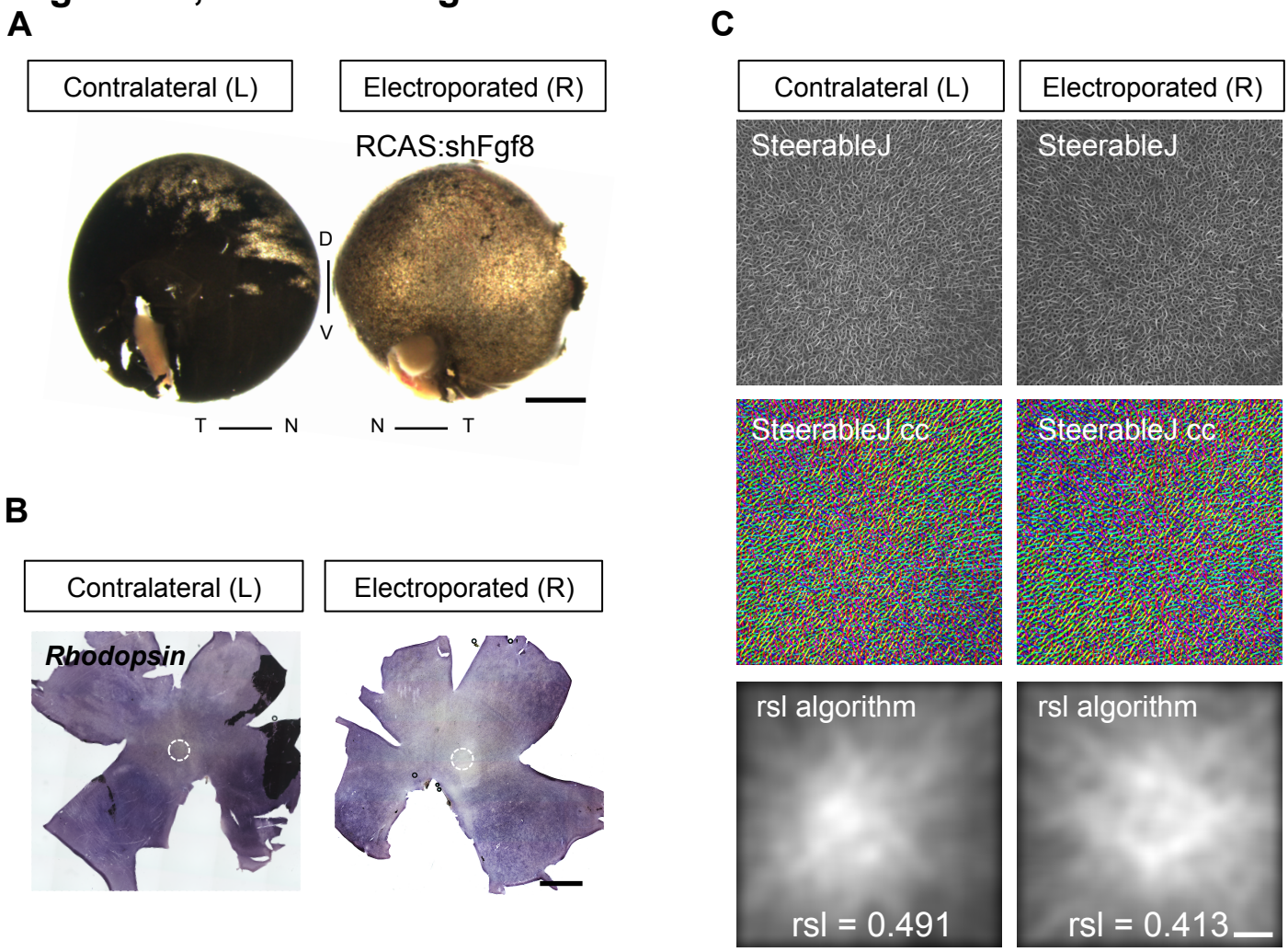

Figure S6- Retinal Fgf8-knockdown by electroporation of RCAS:shFgf8 induced multiple phenotypes in the retina, related to Figure 6

(A) Knockdown of Fgf8 in the retina was accomplished by in vivo electroporation of an shRNA to Fgf8 expressed from the virus, RCAS, as schematized in Figure 6A. Examples of a pair of retinas from the same embryo harvested at E19. Only the right (R) eye was electroporated early at HH11 but due to its replication ability, the virus reached the L eye. Note that Fgf8 knockdown had an effect on RPE pigmentation, with the R eye being completely affected while L eye was only partially affected, as can be seen by the partial RPE depigmentation phenotype, with the dorsal domain being more affected than the ventral region. (B) Rhodopsin flat mount ish on retinas depicted in (A). R retina showed an overall strong downregulation of Rhodopsin ish signal, with some patchiness throughout the whole retina. This effect, and the effect on the RPE, led us to not analyze the RFZ in the R eye, due to potential indirect effects of the changes in the RPE. Dotted circle highlights the RFZ region. (C) The aster structure visualized by SteerableJ or rsl algorithms of a corresponding pair of ipsilateral and contralateral eyes of an RCAS:shFGF8 electroporated embryo. Note that both eyes had an affected aster. Correspondent rsl value for each retina is shown. D, dorsal; V, ventral. N, nasal; T, temporal; Scale bar, 2mm in (A) and (B) and 50μm in (C).

Figure S7, related to Figure 7

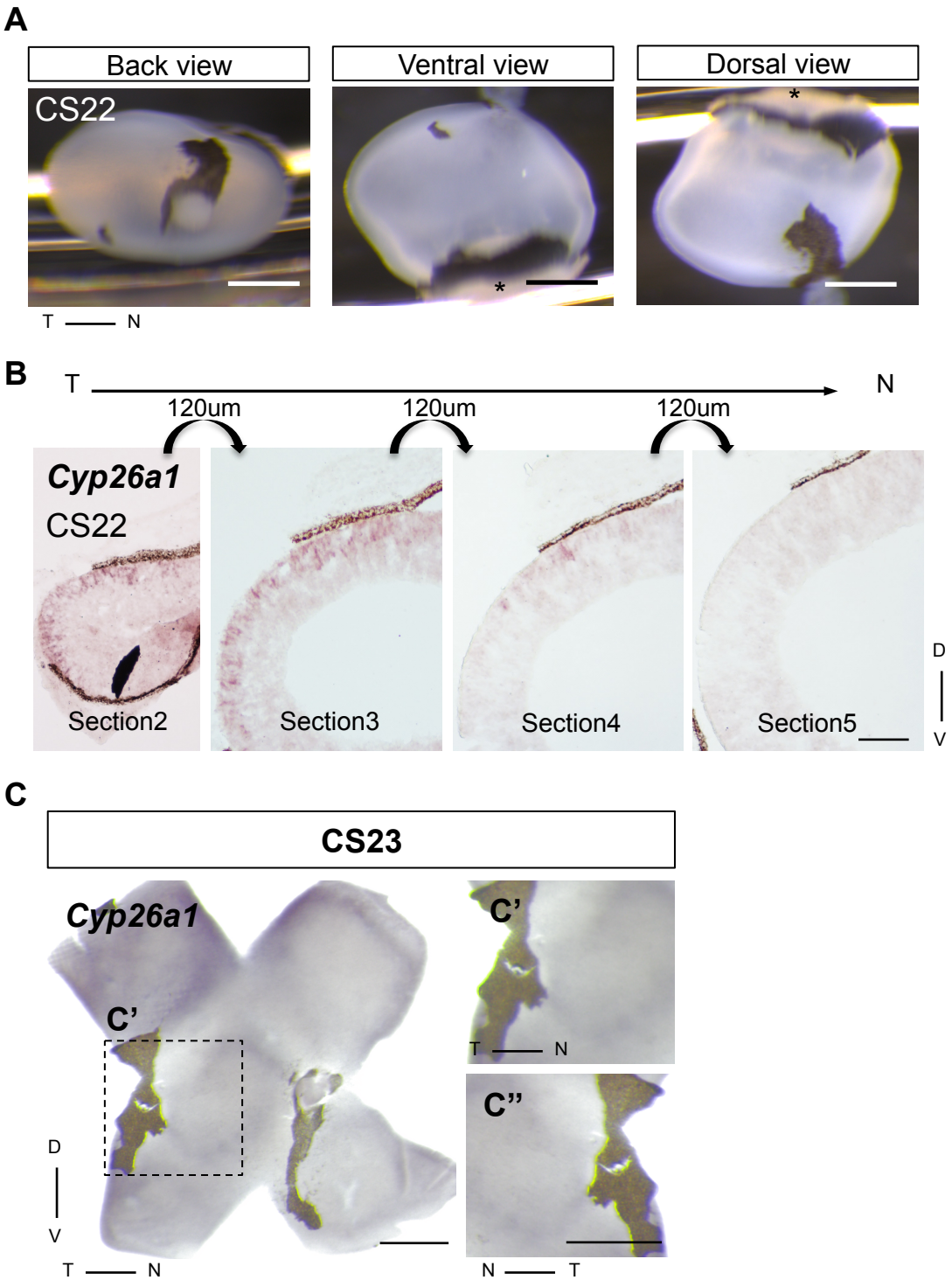

Figure S7 – Cyp26a1 expression in early embryonic human retina, related to Figure 7
(A) Back, ventral and dorsal views of CS22 human embryonic eye illustrating human eye shape at this time in development. (B) Cyp26a1 ish on CS22 retina cross sections along the dorsoventral axis depicting localized signal in only 3 consecutive sections, each 120μm apart. (C) Flat mount ish for Cyp26a1 on CS23 human retina. No ish signal was detected at this stage, only approximately 2 days later than CS22, shown in (B) and Figure 7C-D. Note that since some RPE was still attached to the neural retina in the region of the future fovea, retina was imaged from both outer nuclear layer side (C') and ganglion cell layer side (C") to ensure proper examination, imaging and interpretation of the results. *, lens. Scale bar, 500μm in (A) and (C) and 200μm in (B). D, dorsal; V, ventral; N, nasal; T, temporal.

Table S1- Related to STAR Methods. Additional *ish* probes sequences and qPCR primers

REAGENT or RESOURCE	SOURCE	IDENTIFIER
Sequence-Based Reagents		
Chick Cyp26b1 ish probe tcggcactggctaccctcgcggcgtgcttggtgtcactgactttgctgctggccgtgtcccaac agctgtggcagctccgctgggctgccacccgcgacaaaacctgcaagctaccaatcccta aaggctctatgggattccctttaatcggagaaaccttccactggctcctgcagggttcgtgcttc cagtcttcgcgacgggagaagtacggcaacgtgttcaagacgcacctttttggggcggccg ctggtgagggtgacgggagcggagaacgtgcggaagattctgatgggggaacaccacct ggtgagcaccgaatggccgcgcagcacccgcatgctgctgggacccaacaccgtggcc aactccatcggggacatcca	Based on Reijntjes et al., 2003	N/A
Chick Fgf8 ish probe gctgcagaacgccaagtacgagggctggtacatggccttcacccgcaagggccgcccgc gcaagggctccaagacccggcagcaccaacgcgaggtgcacttcatgaagcggctccc caagggccaccagaccaccgagccccaccggcgcttcgagttcctcaactacccccttcaa ccgcaggagcaaaaggactcgaaactccagcgccagggtgcgcccatgacgcgtgccc ctcggtggactgacgtagagacattgtgatagggttactaaaggaaaaaaaaaacccaac gggggatgggggggaggatacgagaactacatgctctagttgttggtaatgtgggggttgttct gttttt	Vogel et al., 1996	N/A
Chick Rhodopsin ish probe ctacatgttcatgctgatcctgctcggcttccccgtcaacttcctcacgctgtacgtcaccatcc agcacaagaaactccggacgcctctaaactacatcctcctgaacctggtggtcgccgacct ctttatggtctttggaggcttcacgaccaccatgtacacctcgatgaacgggtactttgtctttgg agtaacagggtgctacatcgagggcttctttgctacgc	Bruhn and Cepko, 1996	N/A
Chick PDE6γ ish probe sequence: tgacgcggggcgggctgctagctctgctacagccatgagcttggagccccacaaaccgga gctcaagtcagccaccagggtgaccgggggacccgccacccccgaaaaggaccacct aagttcaagcagaggcagacgcggcaattcaagagcaagccacccaaaaaggggtg caggggtttggcgatgacatcccgggcatggaggggctaggaacagatatcaccgtgatct gcccttgggaagccttcagccacctggagctgcacgagctggcccagtatggcatcat	This paper	N/A
GAPDH F primer: ggatacacagaggaccaggt	This paper	N/A
GAPDH R primer: ccatcaagtccacaacacgg	This paper	N/A
Fgf8 F primer: caagctcatcgtcgag	This paper	N/A
Fgf8 R primer: cgtgtagttgttctcc	This paper	N/A
Cyp26a1 F primer: cctctccaaccttcac	This paper	N/A
Cyp26a1 R primer: cttcacctcgggatac	This paper	N/A
Cyp26c1 F primer: cacagcaccagaactg	This paper	N/A
Cyp26c1 R primer: cagcacctccttgac	This paper	N/A
Raldh1 F primer: gagtgcgcagtggatttgaa	This paper	N/A
Raldh1 R primer: ggcaaaacaggagcaggatt	This paper	N/A
Raldh3 F primer: gaggggtttggaggtgaagt	This paper	N/A
Raldh3 R primer: agttgccaggatgactctgt	This paper	N/A